ELSEVIER

Materials Science and Engineering A 429 (2006) 130–136

MATERIALS SCIENCE & ENGINEERING A

www.elsevier.com/locate/msea

Influence of thermomechanical processing on the superelastic properties of a Ni-rich Nitinol shape memory alloy

D. Favier [a,*], Y. Liu [b], L. Orgéas [a], A. Sandel [a], L. Debove [a], P. Comte-Gaz [c]

[a] Laboratoire Sols-Solides-Structures, Universities of Grenoble (UJF–INPG), UMR CNRS 5521, BP 53, 38041 Grenoble Cedex, France
[b] School of Mechanical Engineering, University of Western Australia, Crawley WA 6009, Australia
[c] Société Minitubes SA, ZAC Technisud, 21 Rue J.Vaujany, BP 2529, F38035 Grenoble Cedex 2, France

Received 5 January 2006; received in revised form 13 April 2006; accepted 3 May 2006

Abstract

Ni-rich NiTi shape memory alloys usually undergo a series of thermomechanical treatment in their production and component fabrication processes. Comprehension of property changes and microstructural evolutions induced by these treatments is essential for quality control and improvement of these materials. The effect of controlled ageing for prolonged times (of the order of several hours) has been extensively investigated in the literature. This study investigates the effect of actual production processes of NiTi tubing, which often involve thermomechanical treatment for multiple periods of short durations and which are typical of industrial production routines of devices like stents, on the transformation and deformation behaviour of a Ti–50.8 at%Ni alloy. Evolution of the properties is characterized by DSC measurements and by tensile testing at 310 K.

Keywords: Martensitic transformation; Heat treatment; Superelasticity; NiTi; Ageing

1. Introduction

Near-equiatomic NiTi alloys, also known as Nitinol, have found growing application in medical stents for implantation in the human body, due to its good corrosion resistance in physiological environments and unique superelastic behaviour compared to the currently used materials of stainless steels. These stents are deployed in application in superelastic state, so to enable instantaneous self-restoration of the designed shape after each pulse contraction. For this purpose stents are usually manufactured using Ni-rich NiTi alloys and certain heat treatment is applied to the final product to optimize the superelastic properties at the human body temperature, commonly an ageing treatment. These stents can be produced either through the expansion of a pattern cut from a small tube or by cutting the deployed design on a tube of a larger diameter [1]. The two manufacturing methods, referred to as the "pre-cut" for the former and "pre-expanded" for the later, are schematically shown in Fig. 1. A single heat treatment at temperatures near 775 K is usually applied in the production of the pre-expanded stents whereas the fabrication of pre-cut stents requires a succession of post-cutting expansion and heat treatment. The single heat treatment for the pre-expanded stents is a simple ageing process, whereas that of the pre-cut stents, on the other hand, is more complicated. The expansion of the cut stents exerts inhomogeneous stress and strain states in different parts of the stent. Correspondingly, ageing under this condition creates the free ageing condition for the straight sections and the constrained ageing condition [2] for the bent joining points of the stent. In a previous study [3], it has been shown by using differential scanning calorimetry (DSC) measurements that the pre-expanded manufacturing process led to a homogeneous two-stage transformation behaviour of $A \rightarrow R \rightarrow M$ of the stent material with a good homogeneity of material properties within each single stent whereas the pre-cut manufacturing process led to inhomogeneous material properties for each single stent.

As processing of medical devices using NiTi often involves thermomechanical treatments, comprehension of property changes and microstructural evolutions induced by these treatments is essential. It is known that most commercial NiTi alloys are Ni-rich and are capable of developing Ti_3Ni_4 precipitates. These fine and coherent precipitates affect both the transformation and mechanical properties of Nitinol [4,5]. Laboratory ageing treatment for prolonged times has been extensively inves-

* Corresponding author. Tel.: +33 4 76 82 70 42; fax: +33 4 76 82 70 43.
E-mail address: Denis.Favier@hmg.inpg.fr (D. Favier).

0921-5093/$ – see front matter
doi:10.1016/j.msea.2006.05.018

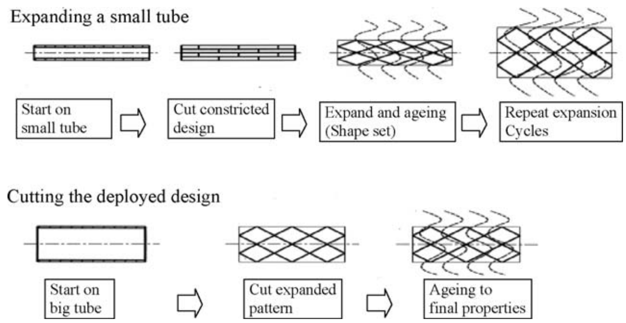

Fig. 1. The pre-cut and the pre-expanded manufacturing routes for the production of stents.

tigated. It has been shown that under certain ageing conditions, Ni-rich NiTi alloys may develop unusual multiple-stage transformation behaviour [6–9]. In the production of the pre-cut stents concerned in this study, three-stage transformation behaviour [3] was observed. The present investigation is concerned with shorter-term thermomechanical treatment processes that are typical of industrial production routines for devices like stents.

2. Experimental procedure

2.1. Material and thermomechanical ageing treatment

Binary Ti–50.8 at%Ni thin-walled tubes of 6 mm inner diameter d_0 and 0.12 mm wall thickness were used in this study. These tubes were produced in straight lengths of several meters by hot drawing with intermediate annealing and final cold drawing by Minitubes SA (France).

Specimens of 115 mm length were cut from these tubes. Ageing treatments were performed by submerging these specimens in a salt bath at 500 °C for various times, followed by quenching into water at room temperature. Two different ageing conditions were used, free ageing and constrained ageing at constant strains. The procedure for the free ageing treatment is illustrated in Fig. 2a. This treatment consisted of one, two or three successive heat treatments at 773 K for times of t_1, t_2, t_3 min for the first, second and third heat treatments, respectively. The procedure of the constrained ageing was more complicated, as shown in Fig. 2b. It constituted of 1, 2 or 3 sequences. Each sequence i started with applying a homogeneous radial strain ε_i, realized by inserting a stainless steel rod of diameter d_i inside the tube at room temperature. Three rod diameters were used: $d_1 = 6.15$ mm, $d_2 = 6.30$ mm and $d_3 = 6.45$ mm, leading to cumulated radial strains of $\varepsilon_1 = 2.5\%$, $\varepsilon_2 = 5\%$ and $\varepsilon_3 = 7.5\%$, respectively. The rod and the tube were then submerged in the salt bath for t_i min. The assembly was then removed from the salt bath at the end of the treatment and quenched in water before the steel rod was removed from the tube.

For the two types of ageing procedures, ageing times t_i ranged from 1 to 5 min leading to cumulated ageing times ranging from 1 to 15 min.

2.2. DSC measurements and tension tests

The transformation behaviour of the aged tubes was studied using DSC. Mechanical behaviour was studied in tensile testing. DSC specimens were cut using a low speed diamond cut-off wheel from aged tubes as thin annular strips of 1.3 mm in width and ~5 mm in length. The samples were cut at 10 mm from the end of tubes to avoid property and microstructure inhomogeneity. Several such strips of total mass of ~20 mg were sealed in Al sample pan to make each sample. The remaining section of

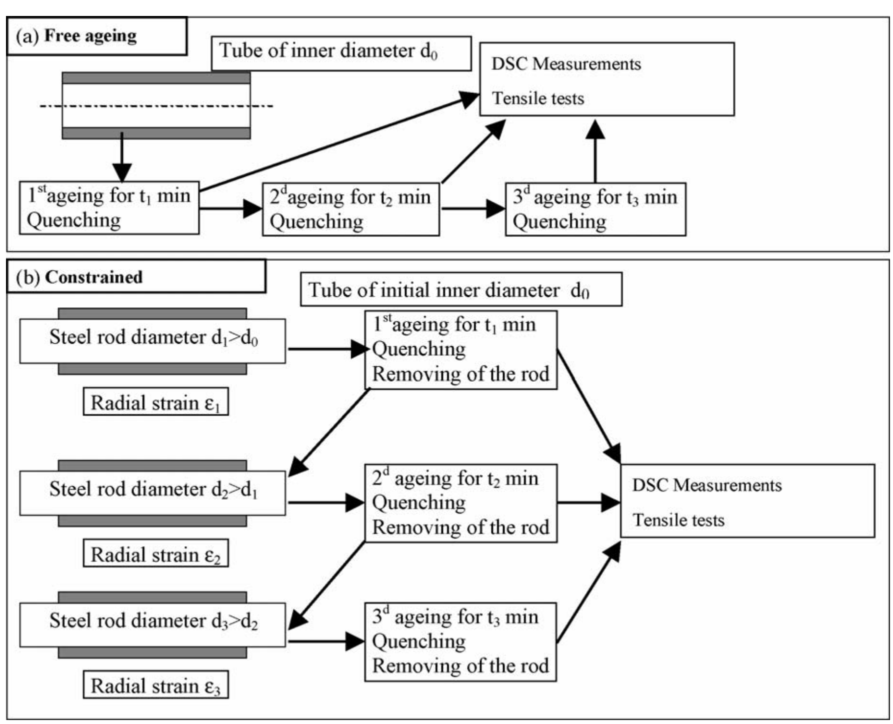

Fig. 2. (a) Free ageing and (b) constrained ageing routines for Nitinol tubes.

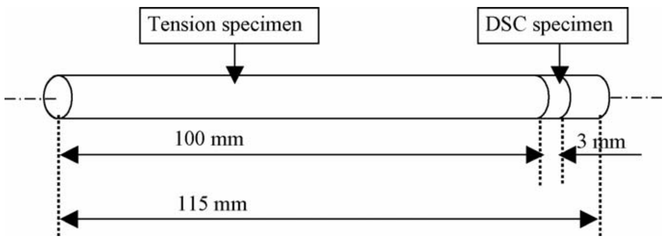

Fig. 3. Sampling of the tension and DSC specimens.

100 mm in length was used as the sample for tensile testing. Due to the gripping system, the gauge length of the tensile sample was approximately 80 mm. The sampling of the tensile and DSC specimens is schematically shown in Fig. 3.

For the DSC measurement, the sample was first equilibrated at 173 K in N atmosphere. The measurement started by heating to 373 K and the heating/cooling rate was 10 K/min. Tensile tests were performed at 310 K in water using a Huber HS 900 ultracryothermostat for temperature control with an accuracy of ±0.2 K [10]. To minimize the thermal effect associated with the martensitic transformation on the mechanical behaviour, all tests were performed with low strain rates of $2 \times 10^{-4}\,s^{-1}$. A grip system has been designed to perform tensile tests of tubes [11].

3. Results

3.1. Thermal transformation—influence of the ageing condition

Fig. 4 shows the thermal transformation behaviour of three specimens. Specimen (a) was in the as-manufactured state. Specimen (b) was after three consecutive free ageing treatments, with $t_1 = t_2 = t_3 = 5$ min. Specimen (c) was after three consecutive constrained ageing treatments, with $\varepsilon_1 = 2.5\%$ and $t_1 = 5$ min, $\varepsilon_2 = 5\%$ and $t_2 = 5$ min, and $\varepsilon_3 = 7.5\%$ and $t_3 = 5$ min. The as-manufactured tube exhibited two transformations on cooling, from austenite to the R phase (A → R) and then from the R phase to martensite (R → M). The reverse transformation on heating also occurred in two steps, from martensite to the R phase (M → R) and then from the R phase to austenite (R → A). The latent heats of the transformations are extremely small, with $\Delta H^{A–R} = 4.15$ J/g and $\Delta H^{R–M} = 1.5$ J/g, as determined for the forward transformations.

The free-aged sample largely preserved the transformation sequence of A → R → M on cooling and M → R → A on heating. However, clear changes are noticeable. The transformation thermal peaks were much enlarged relative to the virgin tube material. The latent heats for the forward transformations were measured to be $\Delta H^{A–R} = 5.15$ J/g and $\Delta H^{R–M} = 6.0$ J/g. In addition, the A → R shifted slightly to a lower temperature whereas the R → M transformation moved higher. The two reverse transformations became much overlapped.

The sample aged under constraint exhibited further evolution in transformation behaviour, despite the fact that the ageing temperature, number of ageing sessions and the total ageing time were identical to those of the free-aged sample. The R → M transformation shifted further to higher temperature and the reverse transformations practically combined into one transformation of M → A, with only a very faint shoulder to the high temperature side, signifying trace amount of the R → A transformation. Latent heats of the transformations were measured to be $\Delta H^{A–R} = 5.25$ J/g and $\Delta H^{R–M} = 7.3$ J/g.

3.2. Superelastic behaviour at 310 K—influence of the ageing condition

Fig. 5 shows the engineering stress–strain curves of the same three tubes as shown in Fig. 4. All three samples showed near complete pseudoelastic recovery after pre-deformation to

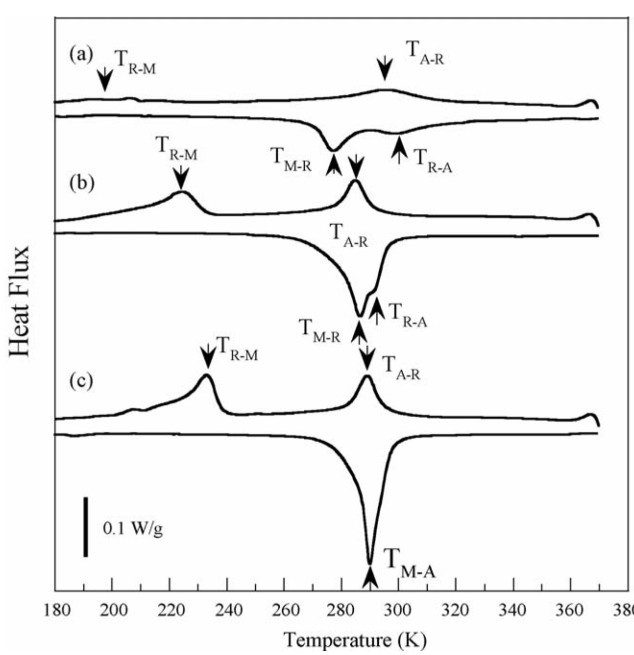

Fig. 4. Transformation behaviour of as-manufactured (a), free-aged (b) and constrained-aged (c) Ti–50.8 at%Ni thin wall tubes (cumulated ageing time of 15 min).

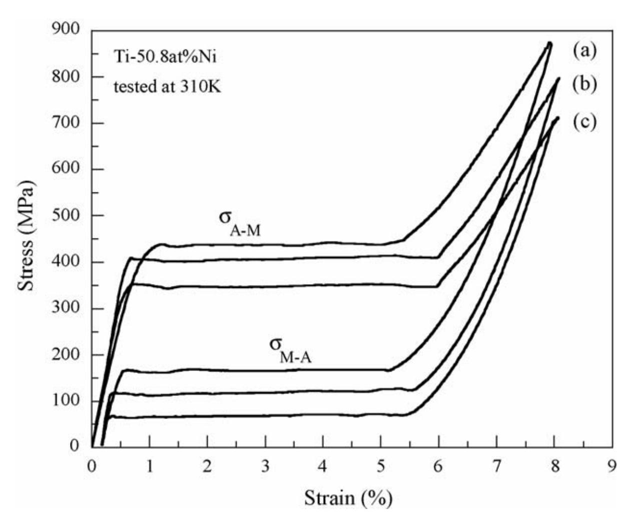

Fig. 5. Superelastic behaviour of as-manufactured (a), free-aged (b) and constrained-aged (c) Ti–50.8 at%Ni thin wall tubes (cumulated ageing time of 15 min).

8% in tension, with near perfect Lüders-type deformation during stress-induced A ↔ M transformation on both loading and unloading. There was no obvious sign of the A ↔ R transformation. The critical stresses for the forward and the reverse transformations were lowered after the ageing treatments, whereas the pseudoelastic hysteresis appeared to remain unchanged, at $\Delta\sigma = 190$ MPa. The continuation of the decreases in the critical stresses from the free-aged sample to the constrained-aged sample is consistent with the continued evolution of the transformation behaviour shown in Fig. 4.

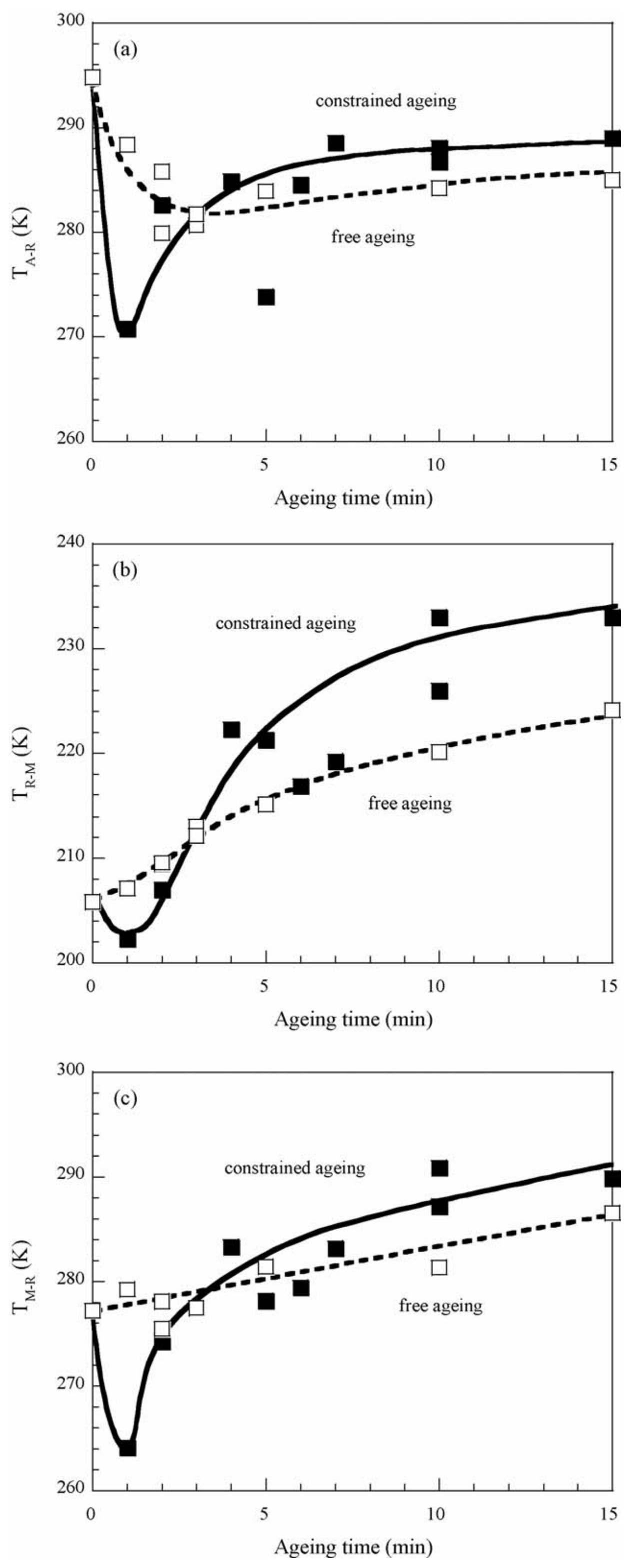

Fig. 6. (a–c) Influence of the cumulated ageing time on the transformation temperatures for free ageing (dashed lines and open squares) and constrained (continuous lines and solid squares) ageing conditions.

3.3. Influence of ageing time on the thermal transformation and superelastic behaviour

Fig. 6 shows the effects of ageing time on the transformation temperatures for the two ageing conditions, with (a) showing T_{A-R}, (b) showing T_{R-M} and (c) showing T_{M-R}. As evident in Fig. 4, there was much overlapping between M → R and R → A transformations, particularly for long ageing times. Therefore, T_{M-R} temperature may also express the T_{M-A} temperature. It is seen that ageing under both the free and constrained conditions caused an immediate decrease of T_{A-R} within the first few minutes. This is believed to be associated with an anneal effect from the virgin state, which contained high density of dislocation. Continued ageing led to a gradual increase of the transformation temperature. T_{R-M}, on the other hand, showed increase with ageing time, as shown in Fig. 6b. This increase occurred after a first initial decrease in the case of constrained ageing. The temperatures of the reverse transformations also increased with increasing ageing time. These observations agree with previous studies and are consistent with the expectation for a decrease in the Ni content in the matrix [7,10]. It is interesting to note that in all three cases, the effect of the constrained ageing appeared to be more pronounced than that of the free ageing.

Fig. 7 shows the effect of ageing time on the critical stresses for the forward and the reverse transformations of the superelasticity. It is seen that in both cases of free ageing and constrained ageing, both the critical stress for the forward transformation, σ_{A-M}, and that for the reverse transformation, σ_{M-A}, decreased with increasing ageing time. These decreases occurred after first

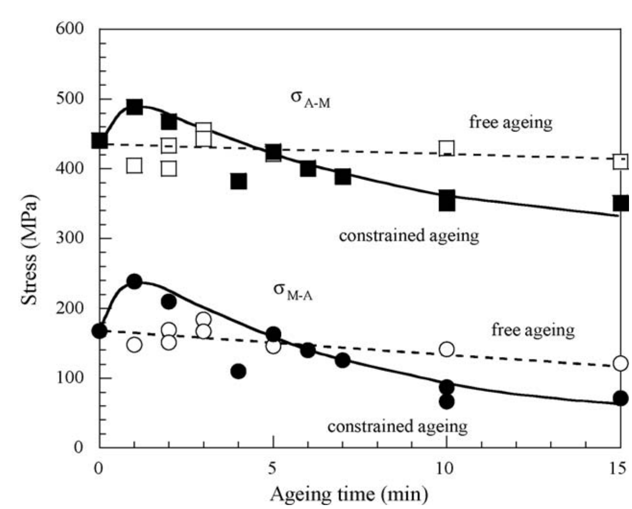

Fig. 7. Influence of the cumulated ageing time on the critical stresses for the forward and the reverse martensitic transformations of superelasticity at 310 K for free ageing (dashed lines and open squares/circles) and constrained ageing (continuous lines and solid squares/circles) conditions.

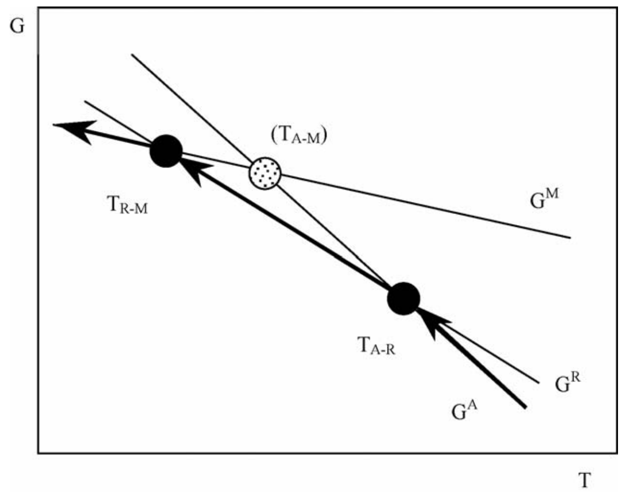

Fig. 8. Thermodynamic expression of the transformation temperatures.

initial increases in the case of constrained ageing. These small increases of the critical stresses at the beginning of ageing for the case under constraint correspond well to the initial decrease of $T_{\mathrm{M-R}}$ shown in Fig. 6. Once again, the decrease of the stresses for the case of constrained ageing was more pronounced than that for the case of free ageing. A decrease in the critical stress for stress-induced martensitic transformation at a given temperature corresponds to an increase in the critical temperature for the corresponding martensitic transformation. In this regard, this observation is consistent with the increases of the critical temperatures for the transformations shown in Fig. 6.

4. Discussion

4.1. Effect of ageing on critical stress for superelasticity

It is evident in Fig. 7 that ageing caused a continuous decrease of the critical stresses for superelasticity. In principle, there exist two possible causes for decrease of the critical stresses of superelasticity at a given temperature: (i) softening of the matrix and (ii) increase of the transformation temperature. The stress–strain curves shown in Fig. 5 indicate that the superelastic deformation proceeded via stress-induced A → M transformation. The DSC measurements shown in Fig. 4 demonstrate that the A → M transformation was prohibited during thermally induced transformation by the A → R → M transformations on cooling. This situation may be schematically illustrated, in thermodynamic context [17], as in Fig. 8. Therefore, direct co-relation between $\sigma_{\mathrm{A-M}}$ determined from the mechanical testing and the corresponding $T_{\mathrm{A-M}}$, which is not measured by DSC, is impossible, hence the differentiation of the two effects mentioned above. However, based on the thermodynamic principles expressed below, $T_{\mathrm{A-M}}$ may be estimated from the measurements of $T_{\mathrm{A-R}}$ and $T_{\mathrm{R-M}}$.

The free energy exchange between the austenite and the martensite may be expressed as:

$$\Delta G^{\mathrm{A-M}} = \Delta H^{\mathrm{A-M}} - T_{\mathrm{A-M}}(S^{\mathrm{M}} - S^{A}). \quad (1)$$

Under the condition that $\Delta G^{\mathrm{A-M}} = 0$, the following relation is established:

$$T_{\mathrm{A-M}} = \frac{\Delta H^{\mathrm{A-M}}}{S^{\mathrm{M}} - S^{\mathrm{A}}} = \frac{\Delta H^{\mathrm{A-M}}}{(S^{\mathrm{M}} - S^{\mathrm{R}}) + (S^{\mathrm{R}} - S^{\mathrm{A}})}. \quad (2)$$

Similarly, the critical temperatures for the A → R and R → M transformation may be expressed as:

$$T_{\mathrm{A-R}} = \frac{\Delta H^{\mathrm{A-R}}}{S^{\mathrm{R}} - S^{\mathrm{A}}}, \quad (3)$$

and

$$T_{\mathrm{R-M}} = \frac{\Delta H^{\mathrm{R-M}}}{S^{\mathrm{M}} - S^{\mathrm{R}}}. \quad (4)$$

Consequently,

$$T_{\mathrm{A-M}} = \frac{\Delta H^{\mathrm{A-M}}}{((\Delta H^{\mathrm{A-R}})/(T_{\mathrm{A-R}})) + ((\Delta H^{\mathrm{R-M}})/(T_{\mathrm{R-M}}))}. \quad (5)$$

The parameters $\Delta H^{\mathrm{A-R}}$, $T_{\mathrm{A-R}}$, $\Delta H^{\mathrm{R-M}}$ and $T_{\mathrm{R-M}}$ are experimentally determined from the DSC measurements. Since enthalpy H is a state function, it follows that $\Delta H^{\mathrm{A-M}} = \Delta H^{\mathrm{A-R}} + \Delta H^{\mathrm{R-M}}$. The $T_{\mathrm{A-M}}$ temperatures calculated using Eq. (5), with $\Delta H^{\mathrm{A-R}} = 6$/Jg and $\Delta H^{\mathrm{R-M}} = 14$/Jg [18], are shown in Fig. 9a

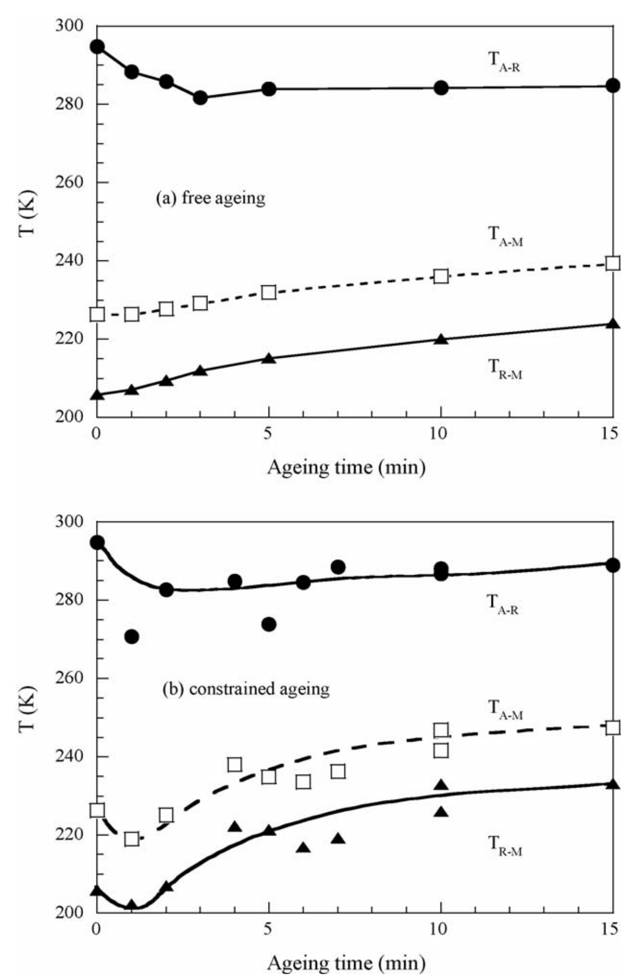

Fig. 9. Critical temperatures $T_{\mathrm{A-M}}$ (open squares) for A → M transformation as calculated according to Eq. (5); (a) free ageing and (b) constrained ageing.

for the free-aged samples and Fig. 9b for the constrained-aged samples. It is seen that $T_{A\text{–}M}$ thus calculated exhibits similar trends of evolution as that of $T_{R\text{–}M}$ in both cases, and appears in between $T_{A\text{–}R}$ and $T_{R\text{–}M}$, as expected.

It is known that the critical stress for stress-induced martensitic transformation at a given temperature is related to the critical temperature of the transformation, or more precisely is linearly dependent on the temperature difference between the testing temperature and the critical transformation temperature, as expressed below:

$$\sigma_{A\text{–}M} = k(T - T_{A\text{–}M}), \qquad (6)$$

where k is the linear constant defined by the Clausius–Clapeyron equation for the martensitic transformation. Using a typical value of $k = 5.5$ MPa/K for precipitation hardened Ni-rich NiTi alloys [11,12], the $\sigma_{A\text{–}M}$ at the testing temperature $T = 310$ K is estimated from (6) and shown in Fig. 10 for both the free-aged and the constrained-aged samples. In the case of free ageing, the calculated curve appears to drop below the experimental curve with increasing ageing time, suggesting an increased effect of matrix strengthening. In the case of constrained ageing, the calculated and the experimentally measured data practically fall onto the same curve, indicating that the evolution of the $T_{A\text{–}M}$ temperature was the cause of the decrease in $\sigma_{A\text{–}M}$ with increasing ageing time.

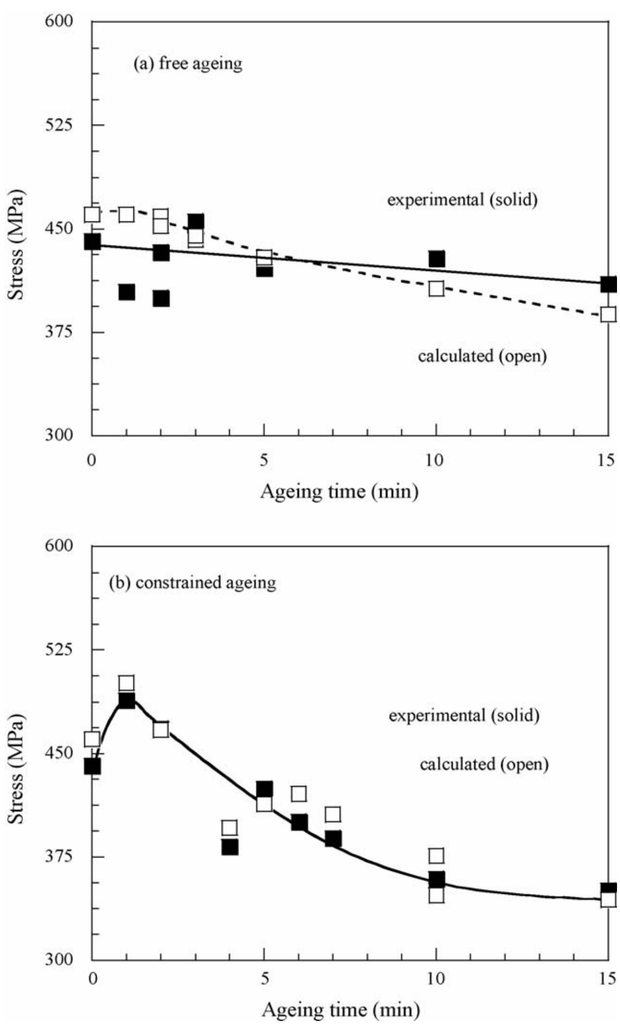

Fig. 10. Critical stress (open square) at testing temperature $T = 310$ K for inducing A → M transformation as estimated according to Eq. (6) from the $T_{A\text{–}M}$ temperature shown in Fig. 9; (a) free ageing and (b) constrained ageing. Comparison with experimental critical stresses (solid squares).

4.2. Comparison between free ageing and constrained ageing

It is seen in Figs. 4–7 that the influences on the transformation and mechanical behaviour of the alloy are stronger for the constrained ageing than for the free ageing. For equal ageing time, the increase of the martensitic transformation temperatures and the corresponding decrease of the transformation stresses are more pronounced for the case of constrained ageing, indicating a faster ageing kinetics. There is very limited information on the direct comparison of ageing kinetics [13] between these two processes in the literature. This observation may be rationalized on the basis of internal stress interaction between the Ti_3Ni_4 precipitates and the applied stress during the constrained ageing. It is known that Ti_3Ni_4 precipitates, which are formed in lenticular shapes, are coherent with the matrix and exert an anisotropic stress field within its vicinity, with a compressive stress in the normal direction of the lenticular discs of the precipitates [14]. An applied stress will encourage the formation of such precipitates preferentially aligned with the external tensile stress perpendicular to the external compressive stress to relax the internal stresses [2,15,16]. In addition, an elastically strained matrix is expected to have faster diffusion rate due to the lattice expansion, which facilitates the faster ageing process in the case of constrained ageing.

5. Conclusions

(1) Ageing Ti–50.8 at%Ni at 773 K for short times of the order of a few minutes led to an increase of the critical temperatures for both R → M and A → M transformations and to a decrease of the critical stress for inducing martensitic transformation at a given temperature.
(2) The decrease of the critical stress was predominantly caused by the increase in the transformation temperatures, instead of softening of the matrix.
(3) For constrained-aged specimen, small initial decreases of the transformation temperatures at the beginning of ageing corresponded well to a small initial increase of the critical stress.
(4) The effects of constrained ageing are more pronounced than those of free ageing.

References

[1] P. Poncin, D. Ferrier, A. Loshakove, J. Proft, C. Meyer-Kobbe, in: S. Russell, A. Pelton (Eds.), Proceedings International Conference on Shape Memory and Superelastic Technologies, Asilomar, California, May, 2000, 2001, p. 477.
[2] M. Nishida, T. Honma, Scr. Met. 18 (1984) 1293.

[3] D. Favier, L. Orgéas, D. Ferrier, P. Poncin, Y. Liu, J. Phys. IV 11 (2001) 541.
[4] S. Miyazaki, T. Imai, Y. Igo, K. Otsuka, Metall. Trans. 17A (1986) 115.
[5] Y.I. Chumlyakov, I.V. Kireeva, V.N. Lineytsev, A.G. Lyisyuk, Mater. Res. Soc. Symp. Proc. 459 (1997) 387.
[6] D. Favier, Y. Liu, P.G. McCormick, Scr. Metall. Mater. 28 (1993) 669.
[7] J.L. Kim, Y. Liu, S. Miyazaki, Acta Mater. 52 (2004) 487.
[8] J. Khalil-Allafi, A. Dlouhy, G. Eggeler, Acta Mater. 50 (2002) 4255.
[9] M. Nishida, T. Hara, T. Ohba, K. Yamaguchi, K. Tanaka, K. Yamauchi, Mater. Trans. JIM 44 (2003) 2631.
[10] L. Orgéas, D. Favier, Acta Mater. 15 (1998) 5579.
[11] A. Sandel, Master's Thesis, University of Grenoble, France, 2000.
[12] G.B. Stachowiak, P.G. McCormick, Acta Mater. 36 (1988) 291.
[13] P. Filip, K. Mazanec, Scr. Mater. 45 (2001) 701.
[14] T. Tadaki, Y. Nakata, K. Shimizu, K. Otsuka, Trans. JIM 27 (1986) 731.
[15] J. Michutta, M.C. Carroll, A. Yawny, Ch. Somsen, K. Neuking, G. Eggeler, Mater. Sci. Eng. A 378 (2004) 152.
[16] L. Bataillard, J.E. Bidaux, R. Gotthardt, Philos. Magn. A 78 (1998) 327.
[17] Y. Liu, P.G. McCormick, Acta Met. 42 (1994) 2401.
[18] Y. Liu, P.G. McCormick, in: Proceedings ICOMAT 92, Monterey, California, 1992, 1993, p. 923.